

Neutral Wind Effect in Producing the Stormtime Ionospheric Additional Layer: Results from Coupled Model Simulations

C. H. Lin¹, A. D. Richmond², J. Y. Liu³, G. J. Bailey⁴

¹Plasma and Space Science Center, National Cheng-Kung University, Tainan, Taiwan, clin@pssc.ncku.edu.tw

²High Altitude Observatory, NCAR, P. O. Box 3000, Boulder, CO 80307, USA, richmond@ucar.edu

³Institute of Space Science, National Central University, Chung-Li 320, Taiwan, jyliu@ss.ncu.edu.tw

⁴Department of Applied Mathematics, University of Sheffield, Sheffield, S3 7RH, UK, G.Bailey@sheffield.ac.uk

Abstract

This study presents theoretical simulation of the low-latitude ionospheric plasma structures during a major magnetic storm. From the coupled NCAR-TIEGCM and SUPIM simulations, stormtime ionospheric additional layers occur in both equatorial and low-latitude regions due to two different physical mechanisms. At equator, the additional layer occurs due to combined effects of penetration electric field and photoionization. Meanwhile, the additional layer formed at low-latitude requires the existence of the disturbance equatorward wind. The results indicate that the ionospheric additional layers may occur in both low-latitude and equatorial regions during magnetic storms if preferable stormtime conditions exist.

1. Introduction

A characteristic feature of the low-latitude ionosphere is the equatorial ionization anomaly (EIA). The EIA morphology is often disturbed due to magnetic-storm disturbances in electric fields, neutral winds, and compositions. The ionospheric additional layers are observed and studied during magnetically quiet period [1]. Some observations also report existence of stormtime additional layer occurred at magnetic equator under strong penetration electric field [2]. However, a comprehensive and theoretical study of physical mechanisms of additional layer formation is missing. It is the purpose of this study to perform a coupled model simulation of the low-latitude ionospheric density structure in order to better understand the physical mechanism of the stormtime ionospheric additional layer.

In this study, The National Center for Atmospheric Research (NCAR) Thermosphere-Ionosphere General-Circulation Model (TIEGCM) [3] is used for simulating the global thermosphere-ionosphere responses to the storm event. The NCAR TIEGCM calculates global distributions of the neutral gas temperature, wind, and

mass mixing ratios of the major and minor constituents. For simulating the October 29-30 storm event, the Assimilative Mapping of Ionospheric Electrodynamics (AMIE) procedure [4], which has inputs from both ground-based and satellite measurements, is used to specify the auroral precipitation and high-latitude convection. Since the TIEGCM has an upper boundary at around 800 km altitude, an ionospheric model that can simulate the low- and mid-latitude ionosphere to greater altitudes is desirable for simulating the enhanced EIA during the storm. We therefore run the Sheffield University Plasmasphere Ionosphere Model (SUPIM)[5], using the TIEGCM neutral winds, temperature, and composition as inputs. In this simulation, 108 field lines with apex altitudes distributed from 150 km to 25000 km are used. Since SUPIM is a two-dimensional model that only simulates the plasmasphere and ionosphere in a single longitudinal sector, we simulate the ionospheric responses to the storm event at -70° geographic longitude ($\sim 4^\circ$ magnetic longitude). The TIEGCM neutral composition, temperature, and winds are interpolated to the SUPIM grid at each time step. The $E \times B$ drifts derived from ROCSAT-1 measurements, as described in section 2, are used to specify field-line convection in SUPIM. The scaled $E \times B$ drifts at 300 km altitude are used for field lines with apex heights between 200 and 600 km, while the scaled $E \times B$ drifts at 2000 km altitude are used for field lines with apex heights between 2000 and 4000 km. Linear interpolation is used for field lines at intermediate apex heights and zero drift is used for the highest and lowest field lines. The $E \times B$ drifts between 4000 km and the altitude of the second outermost field line, 24500 km, are calculated by interpolating the $E \times B$ drift at 4000 km and zero $E \times B$ drift at 25000 km.

2. Results and Discussions

Figure 1 shows the electron density structure for the simulation with inputs of stormtime disturbed electric field and neutral winds but with quiet-time neutral compositions. From Figure 1, the original F_2 layer at the equatorial region has been lifted to above 1500 km altitude. Meanwhile it is seen that the equatorial ionizations are replenished at around 400-500 km altitudes and forming a new ionospheric layer there. At 2200 UT (1718 LT), the strength of electron density at around 500 km altitudes is smaller than those above 1500 km. At this time period, it is possible to observe an additional layer located above the newly formed layer at around 500 km altitude. Ionograms recorded by a digisonde located at Jicamarca show similar feature during the same storm event [6].

Figure 2 shows the simulation with inputs of stormtime disturbed electric field but with quiet-time neutral winds and compositions. The neutral wind (positive southward), field-aligned ion diffusion velocity, and subsequent electron density structure are shown in Figure 2. From the figure, the EIA crests are getting stronger when the strong uplift of the equatorial ionosphere is subsided and a downward diffusion of the plasma from higher to lower altitudes is proceeding. No additional layer is shown in this simulation condition. To evaluate the stormtime neutral wind effects, the disturbed neutral winds are added in the simulation run shown in Figure 3. An apparent signature of the additional layer is clearly seen in Figure 3. Comparing Figures 2 and 3, it is seen that the neutral wind structures are much more complex in Figure 3 and results in significant changes of the field-aligned ion flows. The downward diffusion at latitudes of the EIA crests is slowed down due to existence of equatorward wind.

Meanwhile, at altitudes below EIA crests, the ion flows are controlled by the neutral wind patterns. Poleward/downward ion flows are seen below EIA crests. The differences in the ion flows at different altitudes result in convergence of the ion concentration at the EIA crests. Plasma at the EIA crests drips away slowly to lower altitude and forms a new layer underneath at later times. The process acts like a funnel where the stormtime disturbed neutral wind functions as the narrow neck of the funnel.

3. Summary

In summary, the presented study shows a comprehensive simulation of the stormtime plasma structure at low-latitude and equatorial regions. Results show that the ionospheric additional layer can occur at both equatorial and low-latitude ionosphere with different mechanisms. The additional layer occurred at the equatorial region is formed due to a strong uplift of the original F₂ layer results from an eastward penetration electric field, followed by replenishment of the newly produced ionization located at the original F₂ layer height. This process requires existence of the sunlight in order to produce fresh plasma through photoionization process. On the other hand, the additional layer formed at low-latitude requires the existence of the storm-generated equatorward wind. The storm-generated equatorward wind slows down the downward diffusion of plasma at the equatorial ionization anomaly (EIA) crests. Dripping down of the EIA plasma to lower altitudes forms a new additional layer. The stormtime equatorward neutral wind plays a critical role in production of the additional layer at latitudes of EIA crests.

4. References

1. Balan, N., I. S. Batista, M. A. Abdu, J. MacDougall, and G. J. Bailey, Physical mechanism and statistics of occurrence of an additional layer in the equatorial ionosphere, *J. Geophys. Res.*, **103(A12)**, 1998, pp. 29169–29181.
2. Paznukhov, V. V., B. W. Reinisch, P. Song, X. Huang, T. W. Bullett, and O. Vellz, Formation of an F3 layer in the equatorial ionosphere: A result from strong IMF changes, *J. Atmos. Sol. Terr. Phys.*, **69**, 2007, pp. 1292-1304.
3. Richmond, A. D., E. C. Ridley, and R. G. Roble, A Thermosphere/Ionosphere General Circulation Model with Coupled Electrodynamics, *Geophys. Res. Lett.*, **19(6)**, 1992, pp. 601–604.
4. Richmond, A. D., and Y. Kamide, Mapping Electrodynamical Features of the High-Latitude Ionosphere from Localized Observations: Technique, *J. Geophys. Res.*, **93(A6)**, 1988, pp. 5741–5759.
5. Bailey, G. J., and N. Balan, A Low-Latitude Ionosphere-Plasmasphere Model, in *Solar-Terrestrial Energy Program: Handbook of Ionospheric Models*, edited by R. W. Schunk, 1996.
6. Zhao, B. W. Wan, and L. Liu, Responses of equatorial anomaly to the October-November 2003 superstorms, *Ann. Geophysicae*, **23**, 2005, pp. 693-706.

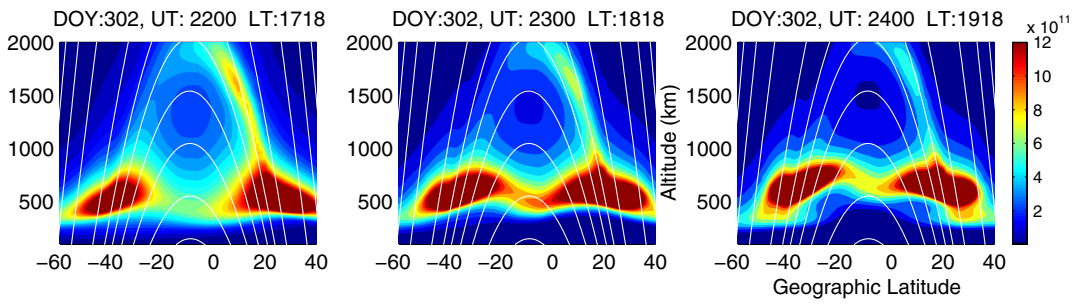


Figure 1. Simulation result showing formation of additional layer at equator.

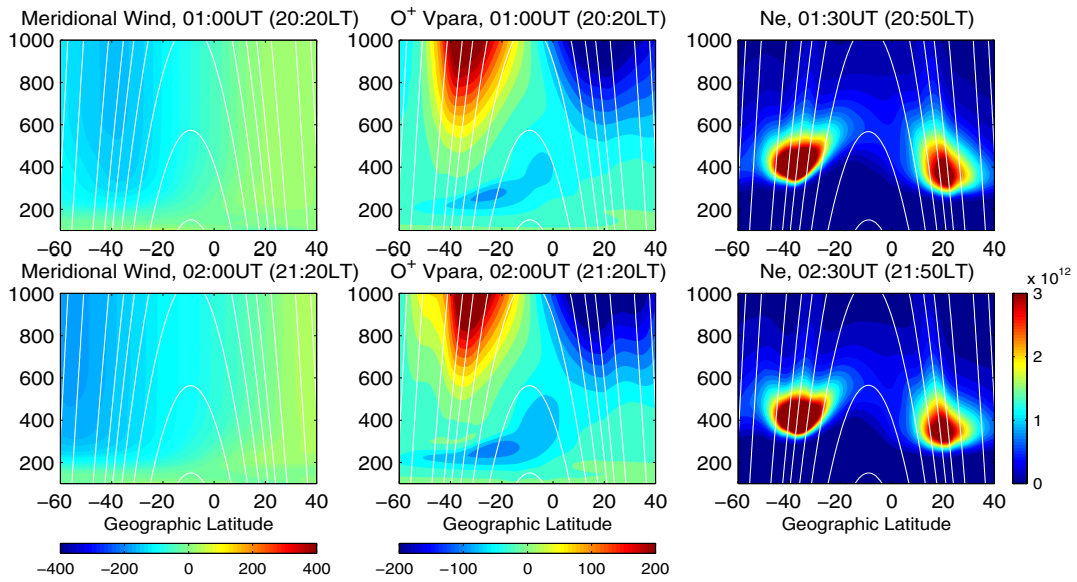


Figure 2. Simulation result showing no additional layer at EIA crests if stormtime equatorward winds are not included.

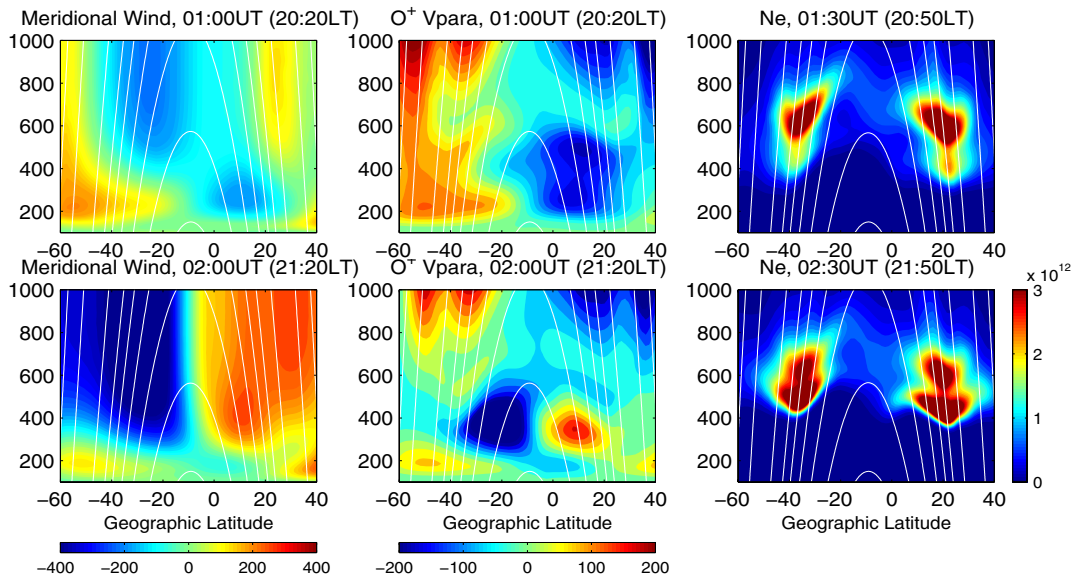


Figure 3. Simulation result showing formation of additional layer at EIA crests.